

DATA MINING: ANALYSIS OF THE HQM AND JOMPQ LIGHT CURVES OF AGNs



B. Mihov, L. Slavcheva-Mihova

Institute of Astronomy and NAO, Bulgarian Academy of Sciences, Sofia, Bulgaria

Introduction

Quasars are variable on different time scales and with various amplitudes. Their variability has been extensively explored for several decades. Quasar variability studies could provide limits on the size of the emitting regions, could constrain emission models, and could probe the physical conditions in the vicinity of the supermassive black hole. However, the successful usage of the flux variations for analysis of the physical processes in quasars requires well sampled and highly accurate light curves.

A good example in this context is the Hamburg Quasar Monitoring Programme (HQM) run on the 1.23-m telescope of the Calar Alto Observatory, Spain, between 1988 and 1995 (Borgeest & Schramm 1994; Schramm et al. 1994a,b). In the course of HQM it was realized that light curves with a very good sampling can be obtained either by using a dedicated telescope at an excellent site or by having a cooperation among different observatories at different longitudes around the world. In 1994 an international monitoring collaboration was created with the aim to produce densely sampled light curves of quasars – the so called Joint Optical Monitoring Programme of Quasars (JOMPQ; Schramm et al. 1994c). A sample of quasars was selected to be observed as often as possible; for a subsample joint observations “around the clock” were scheduled. The first two campaigns took place in September 1994 and January/February 1995. Unfortunately, soon afterwards the programme was ceased.

We started analysis of the HQM/JOMPQ light curves having good time coverage. To achieve this we used the sampling rate of a set of not equally sampled data (Borgeest & Schramm 1994) generally larger than 5. In some occasions lower sampling rates were used. For this study we selected the following blazars: 0420-014, 1641+399, and 2251+158. Their HQM/JOMPQ light curves were downloaded and nightly binned: the magnitudes were weight-averaged and the MJDs – median-averaged.

Comments on Individual Objects

0420-014 The object was observed from Nov 9, 1988 to Feb 23, 2001 in a total of 124 nights. The long-term variability amplitude, defined in Heidt & Wagner (1996), for this period is 3.80 mag. The weighted mean blazar magnitude is 16.16±0.07 with a weighted standard deviation of 0.79 mag. If we assume that the long-term variability is caused by the Doppler factor variations, then the quoted variability amplitude requires a Doppler factor change of 5.8 times (see Sadun et al. 2018 for relevant formulae). During the JOMPQ campaign, Jan 23 – Feb 2, 1995, a steady brightness decrease was observed (Fig. 1). The linear approximation resulted in a slope of 61±2 mmag/day if the fit is weighted and 60±3 mmag/day otherwise. In the framework of the geometric origin of the blazar variability, this linear trend can be caused by the viewing angle decrease with a rate of 0.190°/day and 0.187°/day, respectively (see Montagni et al. 2006 for the corresponding formulae). The maximum apparent velocity needed for this calculation is taken from Liodakis et al. (2018).

1641+399 The object was observed from Sep 5, 1988 to Feb 24, 2001 in a total of 246 nights. The long-term variability amplitude for this period is 3.14 mag. The weighted mean magnitude is 16.47±0.03 with a weighted standard deviation of 0.32 mag. If we assume that the long-term variability is caused by the Doppler factor variations, then the quoted variability amplitude requires a Doppler factor change of 4.2 times. The source showed three flares of $\Delta m \sim 3$ mag modeled in Schramm et al. (1993) by means of a “light-house” effect. Aside from these flares, the most intriguing feature is a pre-flare on the “shoulder”, preceding the second flare (Fig. 2). The pre-flare was observed during Jul-Aug 1991. Its colour-magnitude diagram (CMD) shows clear redder-when-brighter (RWB) chromatism; the linear fit has a slope of -0.42±0.06 and a linear correlation coefficient of -0.94 with corresponding p -value ~ 0.00001 (Fig. 3). The overall CMD (see Schramm et al. 1993, Mihov et al. 2008) also shows RWB chromatism but for magnitudes brighter than ~ 15.5 the variations become achromatic. A possible explanation is that at these flux levels the Doppler boosted emission of the blob/shock, which moves on a helical trajectory and causes the flaring, dominates the overall RWB emission of the jet. This RWB trend could be explained with a generally redder emission of the jet compared to that of the accretion disk, which causes reddening as the jet gets brighter. We approximated the pre-flare with a double exponential law (Abdo et al. 2010) plus a linear base level. The rise and decay e -folding time scales are $T_{\text{rise}} = 2.1 \pm 0.3$ day and $T_{\text{decay}} = 7.6 \pm 1.9$ day (as measured in the observer frame), so, the flare is asymmetric, which rules out its geometric origin. The estimates of the time scales allow us to compute some parameters of the emitting region.

The upper limit of the region radius could be found as $R \leq c T_{\text{rise}} \delta / (1+z)$, where c is the speed of light and δ the Doppler factor. We adopted $\delta = 4.63$ (+4.65/-1.68) from Liodakis et al. (2018) and found $R \leq (1.6 + 1.6/-0.6) \times 10^{16}$ cm. Radii of this order are typically assumed as the jet radius in spectral energy distribution modeling of blazars (Chen 2018).

As we noted, the pre-flare is asymmetric. If we assume that (i) the flare is caused by the synchrotron emission of electrons, which cool after being accelerated at the front of a shock and (ii) the injection of accelerated particles in the emitting region takes place in time scales less than the light crossing one, then the asymmetry means that the cooling time scale is longer than the light crossing one, $T_{\text{cool}} \geq R/c$. Therefore, we can put limits on the magnetic field strength and the electron energy in the flare region (Ghisellini et al. 1997). We further assume equipartition of the magnetic energy density and the synchrotron radiation energy density (as measured in the comoving frame). We obtained the following limits: $B \leq (0.10 + 0.05/-0.03)$ Gauss and $\gamma_0 \geq (2.0 + 1.0/-0.4) \times 10^4$, where γ_0 is the energy of the electrons (in units of mc^2), emitting in the Johnson R band. These limits, however, are extreme for flat-spectrum radio-quasars (see Chen 2018).

The pre-flare occurs on the top of a lineary brightening trend of a slope of -15±1 mmag/day, which translates into a viewing angle decrease rate of 0.014°/day. The structure function of the de-trended pre-flare is shown in Fig. 4 – its slope is 1.27±0.22. If we assume that the flaring is caused by a shock moving on a helical path down the jet, then the pre-flare could result from a turbulent region energized by the shock and then cooled by a synchrotron emission.

2251+158 The object was observed from Jul 31, 1990 to Sep 06, 2000 in a total of 67 nights. The long-term variability amplitude for this period is 1.17 mag. The weighted mean magnitude is 15.92±0.03 with a weighted standard deviation of 0.24 mag. If we assume that the long-term variability is caused by the Doppler factor variations then the quoted variability amplitude requires a Doppler factor change of 1.7 times. During the JOMPQ campaign Sep 1-10, 1994 a steady brightness increase was observed (Fig. 5). The linear approximation resulted in a slope of -6.2±1.2 mmag/day if the fit is weighted and -9.9±1.5 mmag/day otherwise. In the framework of the geometric origin of the blazar variability this linear trend is caused by the viewing angle increase with a rate of 0.008°/day and 0.012°/day, respectively.

References

Abdo, A. A., et al. 2010, ApJ, 722, 520
Borgeest, U., Schramm, K.-J. 1994, A&A 284, 764
Chen, L. 2018, ApJS, 235, 39
Ghisellini G. Villata M. Raiteri C. M. et al. 1997 A&A, 327 61
Heidt, J. & Wagner, S. J. 1996, A&A, 305, 42
Liodakis, I., et al. 2018, ApJ, 866, 137
Mihov, B., et al. 2008, AN, 329, 77
Montagni, F., et al. 2006, A&A, 451, 435
Sadun, A. C., et al. 2018, Galaxies, 6, 20
Schramm, K.-J., et al. 1993, A&A, 278, 391
Schramm, K.-J., et al. 1994a, A&AS, 104, 473
Schramm, K.-J., et al. 1994b, A&AS, 106, 349
Schramm, K.-J., et al. 1994c, Publ. Beijing Astron. Obs, 25, 1

This research is based on activities partially supported by the Bulgarian National Science Fund under contract DN 18/13-12.12.2017 and within the agreement between the Bulgarian and Serbian academies of sciences for the period 2020 – 2022.

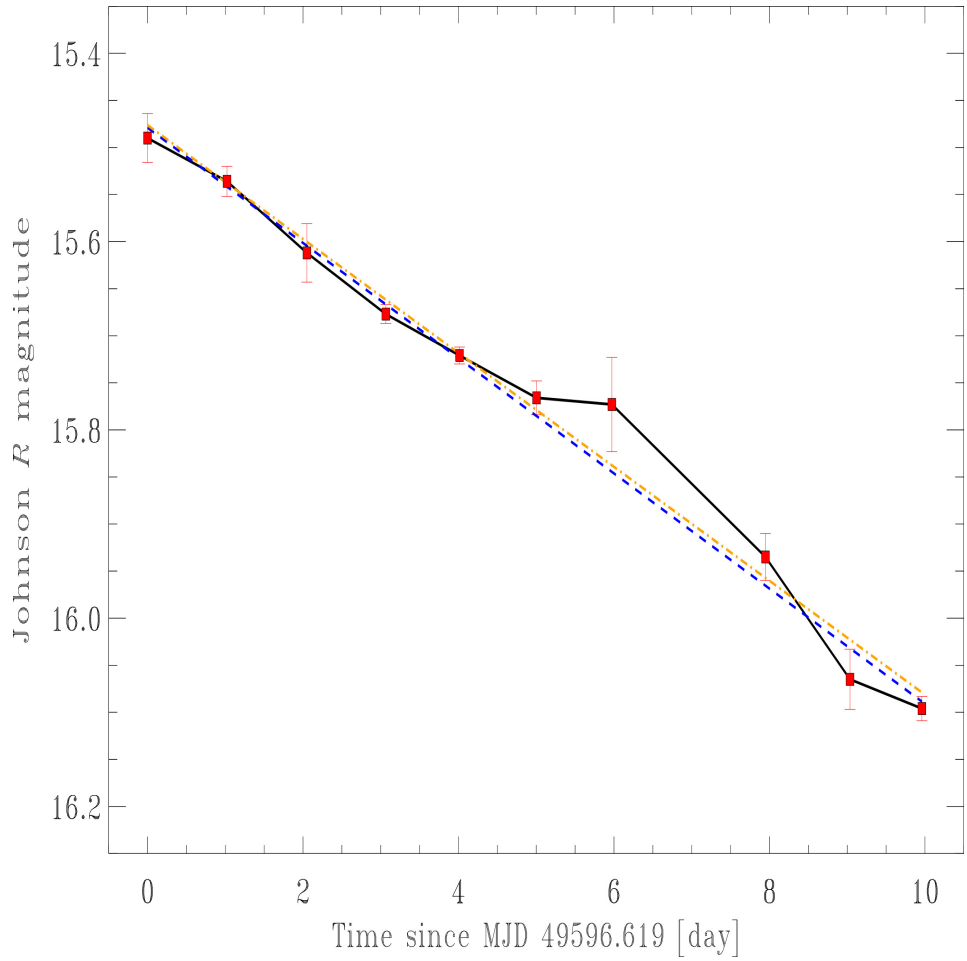


Fig. 1: Linear fit for 0420-014.

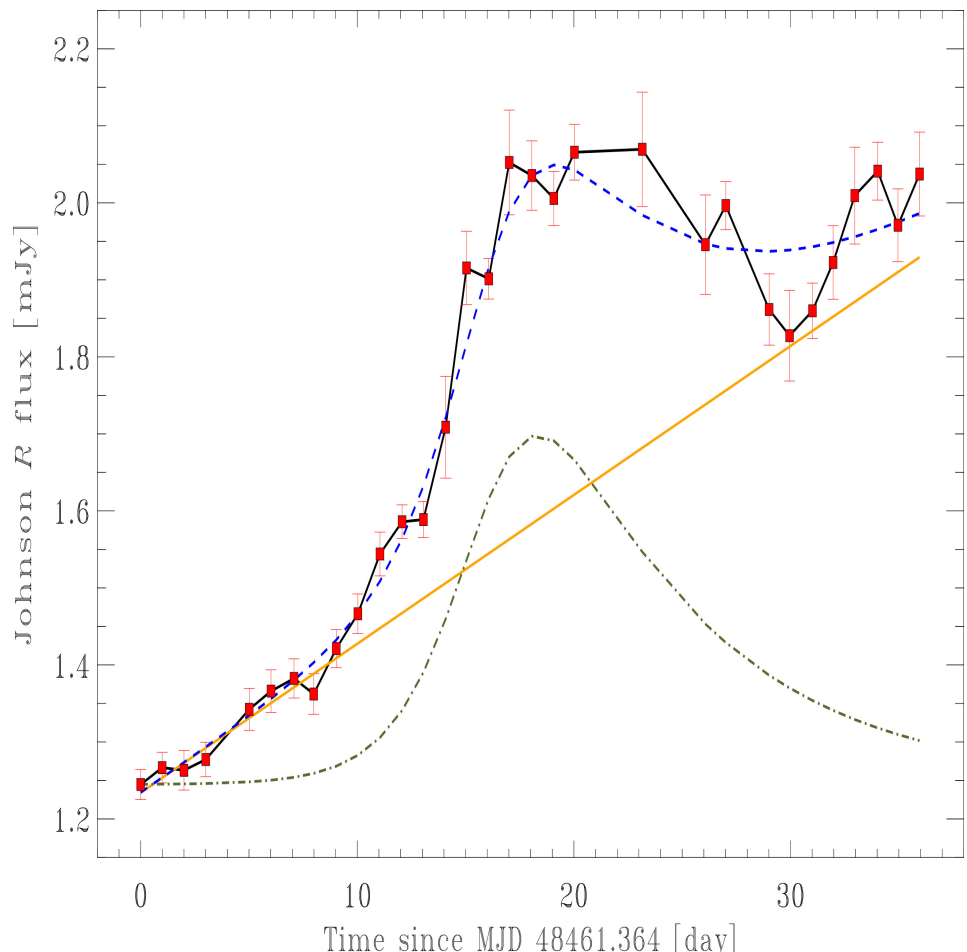


Fig. 2: Pre-flare decomposition for 1641+399.

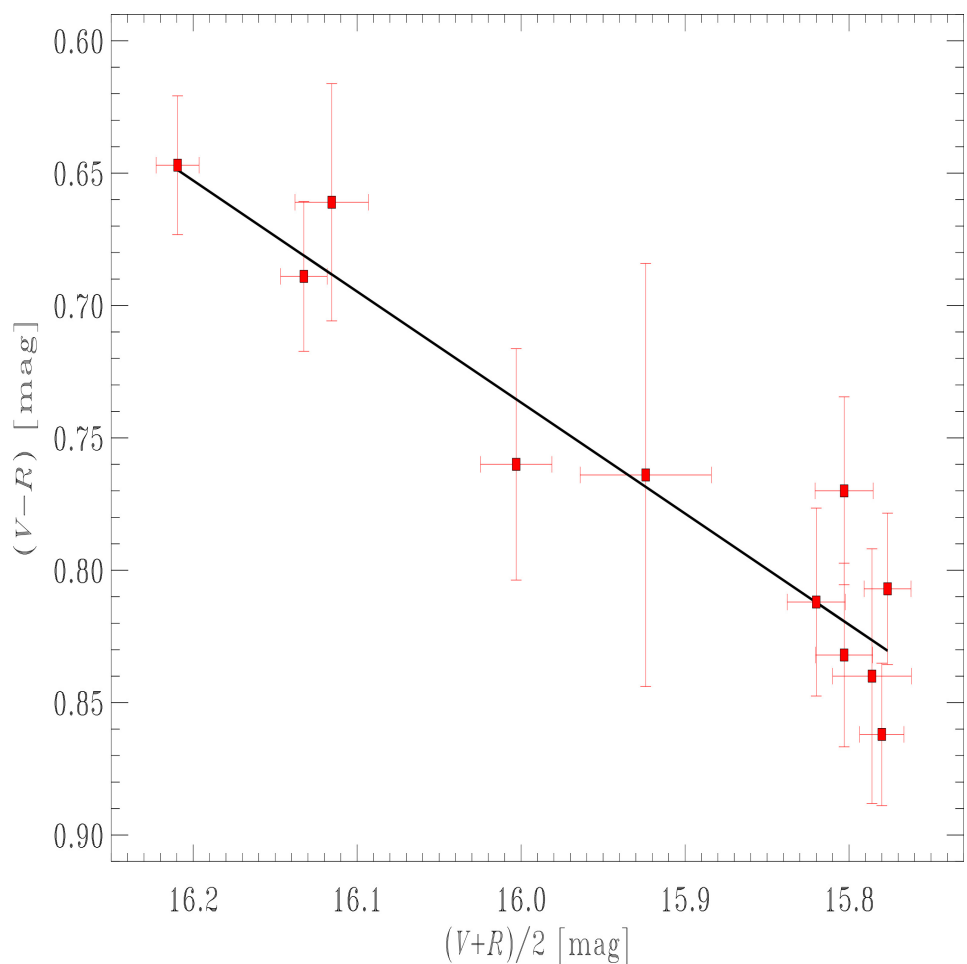


Fig. 3: CMD for the pre-flare of 1641+399.

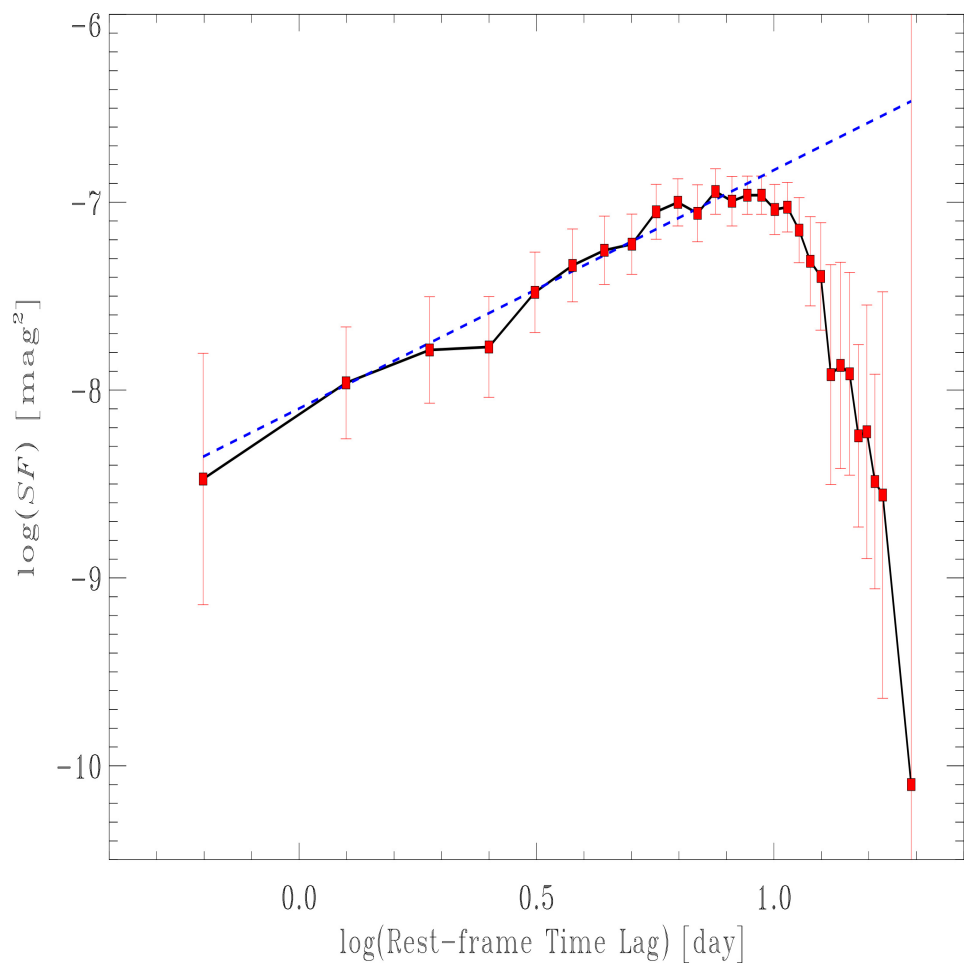


Fig. 4: SF for the de-trended pre-flare of 1641+399.

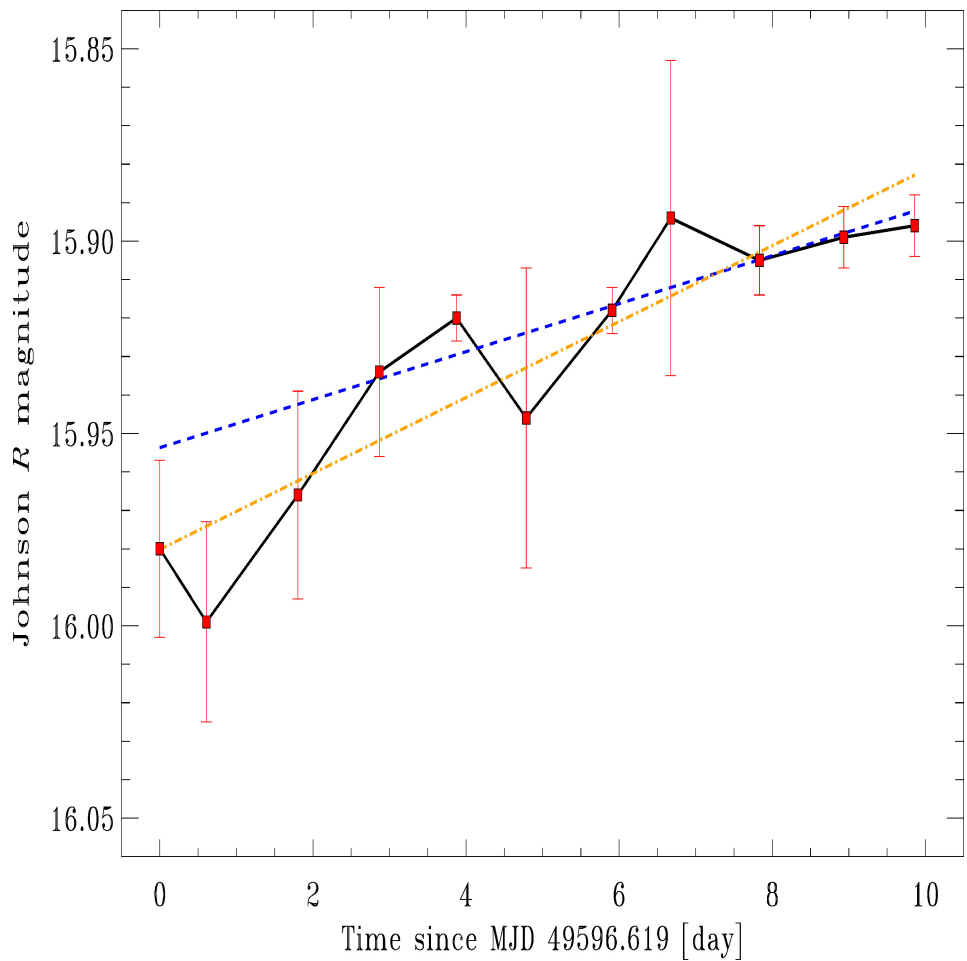


Fig. 5: Linear fit for 2251+158.